Since January 2020 Elsevier has created a COVID-19 resource centre with free information in English and Mandarin on the novel coronavirus COVID-19. The COVID-19 resource centre is hosted on Elsevier Connect, the company's public news and information website.

Virology 568 (2022) 13–22

Contents lists available at ScienceDirect

Virology

journal homepage: www.elsevier.com/locate/virology

SARS-CoV-2 viroporin encoded by *ORF3a* triggers the NLRP3 inflammatory pathway

Huanzhou Xu [a], Ibukun A. Akinyemi [b], Siddhi A. Chitre [a], Julia C. Loeb [c,d], John A. Lednicky [c,d], Michael T. McIntosh [b,e], Sumita Bhaduri-McIntosh [a,e,*]

[a] Division of Infectious Disease, Department of Pediatrics, University of Florida, Gainesville, FL, USA
[b] Child Health Research Institute, Department of Pediatrics, University of Florida, Gainesville, FL, USA
[c] Department of Environmental and Global Health, College of Public Health and Health Professions, University of Florida, Gainesville, FL, USA
[d] Emerging Pathogens Institute, University of Florida, Gainesville, FL, USA
[e] Department of Molecular Genetics and Microbiology, University of Florida, Gainesville, FL, USA

ARTICLE INFO

Keywords:
SARS-CoV-2
COVID-19
NLRP3 inflammasome
ORF3a
Viroporin
Cytokine
Antiviral

ABSTRACT

Heightened inflammatory response is a prominent feature of severe COVID-19 disease. We report that the SARS-CoV-2 ORF3a viroporin activates the NLRP3 inflammasome, the most promiscuous of known inflammasomes. Ectopically expressed ORF3a triggers IL-1β expression via NFκB, thus priming the inflammasome. ORF3a also activates the NLRP3 inflammasome but not NLRP1 or NLRC4, resulting in maturation of IL-1β and cleavage/activation of Gasdermin. Notably, ORF3a activates the NLRP3 inflammasome via both ASC-dependent and -independent modes. This inflammasome activation requires efflux of potassium ions and oligomerization between the kinase NEK7 and NLRP3. Importantly, infection of epithelial cells with SARS-CoV-2 similarly activates the NLRP3 inflammasome. With the NLRP3 inhibitor MCC950 and select FDA-approved oral drugs able to block ORF3a-mediated inflammasome activation, as well as key ORF3a amino acid residues needed for virus release and inflammasome activation conserved in the new variants of SARS-CoV-2 isolates across continents, ORF3a and NLRP3 present prime targets for intervention.

1. Introduction

Effective management of severely ill individuals requires immune modulatory strategies. Indeed, during the second week of illness, many individuals experience an inflammatory surge that can herald severe disease (Liu et al., 2020; Mehta et al., 2020). This inflammatory response, composed of IL-1β and other cytokines, results from assembly/activation of a multiprotein host machinery known as the inflammasome in both immune and non-immune cells such as airway epithelial cells – the most prominent is the NLRP3 (NOD-, LRR- and pyrin domain-containing protein 3)-inflammasome – and several lines of evidence tie activation of the NLRP3-inflammasome to severe SARS-CoV-2 pathology, including i) individuals with comorbidities such as diabetes, atherosclerosis, and obesity (all pro-inflammatory conditions marked by NLRP3 activation) (Chen et al., 2017; Dixit, 2013; Grant; Dixit, 2013; Jin and Fu, 2019; Rheinheimer et al., 2017; Stienstra et al., 2011) are at greater risk for severe disease (Richardson et al., 2020; Wu and McGoogan, 2020; Yang et al., 2020), ii) viroporins expressed by the closely-related SARS-CoV activate the NLRP3 inflammasome (Chen et al., 2019; Nieto-Torres et al., 2014, 2015; Siu et al., 2019), and iii) bats, the asymptomatic reservoir of CoVs that are highly pathogenic in humans, are naturally defective in activating the NLRP3-inflammasome (Ahn et al., 2019). Although cellular ACE2 engagement by SARS-CoV-2 spike protein can cause expression of pro-inflammatory genes (Ratajczak et al., 2020), whether and how SARS-CoV-2 activates the inflammasome remains relatively unexplored. Reviews in the literature also speculate on the importance of targeting the inflammasome (de Rivero Vaccari et al., 2020; Freeman and Swartz, 2020). Indeed, investigations into SARS-CoV-2-inflammasome mechanisms to identify therapeutic targets are now especially relevant as the virus has demonstrated its ability to mutate, raising concerns about the efficacy of newly developed vaccines and antivirals that may target the virus (Baric, 2020; Moore and Offit, 2021).

We investigated the influence of the SARS-CoV-2 viroporin ORF3a, a highly conserved CoV protein that facilitates virus release, on the NLRP3 inflammasome. Viroporins are virus-encoded proteins that are

* Corresponding author.Division of Infectious Disease, Department of Pediatrics, University of Florida, Gainesville, FL, USA
E-mail address: sbhadurimcintosh@ufl.edu (S. Bhaduri-McIntosh).

https://doi.org/10.1016/j.virol.2022.01.003
Received 11 October 2021; Received in revised form 11 January 2022; Accepted 12 January 2022
Available online 17 January 2022

considered virulence factors. Though typically not essential for virus replication per se, some of these hydrophobic proteins can form pores that facilitate ion transport across cell membranes, and by doing so, ensure virus release with the potential for coincident inflammasome activation (Farag et al., 2020; He et al., 2016; Nieto-Torres et al., 2015; Nieva et al., 2012). A component of the innate immune system, the inflammasome assembles and responds to invading organisms, thus forming the first line of defense against infections (Broz and Dixit, 2016). Our experiments show that compared to the two other putative SARS-CoV-2 viroporins encoded by *ORF-E* and *ORF-8*, ORF3a protein primes and potently activates the inflammasome via efflux of potassium ions and the kinase NEK7. Its ability to activate caspase 1, the central mediator of proinflammatory responses, depends on NLRP3 since a selective inhibitor of NLRP3 blocks this pathway in infected cells. We also report that three oral medications (an antimicrobial, an antidiabetic, and an anticancer drug), all of which target the NLRP3 inflammasome and ameliorate inflammatory conditions (Ito et al., 2015; Liu et al., 2017; Tsuji et al., 2020; Wang et al., 2017; Xu et al., 2019b; Yang et al., 2019; Zhang et al., 2017), block ORF3a-mediated inflammasome activation. Finally, we find that although the SARS-CoV-2 ORF3a protein has diverged somewhat from its homologs in other CoVs, some of these newly divergent residues are essential for activating the NLRP3 inflammasome and are perfectly conserved in virus isolates across continents, including the recently emerged highly infectious variants.

2. Results

2.1. SARS-CoV-2 viroporin ORF3a primes and activates the inflammasome, triggering cell death

With lung as the predominant site of pathology along with established tropism for kidney and other organs (Puelles et al., 2020), we introduced ORF3a into lung origin A549 cells and for comparison, kidney origin HEK-293T cells, cell types that support SARS-CoV-2 infection (Hoffmann et al., 2020), and found induction of pro-IL-1β transcripts and protein, consistent with priming of the inflammasome. Compared to empty vector-exposed cells, ORF3a protein also increased the levels of cleaved, i.e. the active form of the pro-inflammatory caspase, caspase 1, as well as the cleaved form of the caspase 1 substrate, pro-IL-1β, indicating activation of the inflammasome, again in both cell types (Fig. 1A). Priming by ORF3a protein resulted in increased expression of *IL-1β* message (Fig. 1B) likely due to NFκB-mediated mechanisms as indicated by increased IκBα phosphorylation (Fig. 1C), reduced abundance of IκBα (Fig. 1C), and enrichment of NFκB p65 at the *IL-1β* promoter (Fig. 1D) despite no change in abundance of p65 in ORF3a protein expressing cells (Fig. 1E). ORF3a protein also caused cleavage/activation of Gasdermin D, the pyroptosis-inducing caspase 1-substrate, indicated by an increase in the N-terminal fragment of Gasdermin D (Fig. 1F). This was accompanied by ORF3a protein-mediated increased cleavage/activation of caspase 3 (Fig. 1G) and cell death (Fig. 1H), likely secondary to both pyroptosis and apoptosis, indicated by increased levels of GSDMD-N and cleaved caspase-3, respectively (Fig. 1F and G). We also expressed the two other putative viroporins encoded by *ORF-E* and *ORF-8* and found that they triggered caspase 1 cleavage less robustly than ORF3a (Fig. 1I); this modest activation of caspase 1 may be due to suboptimal transfection efficiency and expression of ORF-E and ORF-8 proteins (Fig. 1J). Thus, ORF3a protein primes the inflammasome by triggering NFκB-mediated expression of pro-IL-1β while also activating the inflammasome to cleave pro-caspase 1, pro-IL-1β, and the pore-forming Gasdermin D, inducing cell death.

2.2. ORF3a protein activates the NEK7-NLRP3 inflammasome via ASC-dependent and independent modes

In probing the mechanism of ORF3a protein-mediated activation of

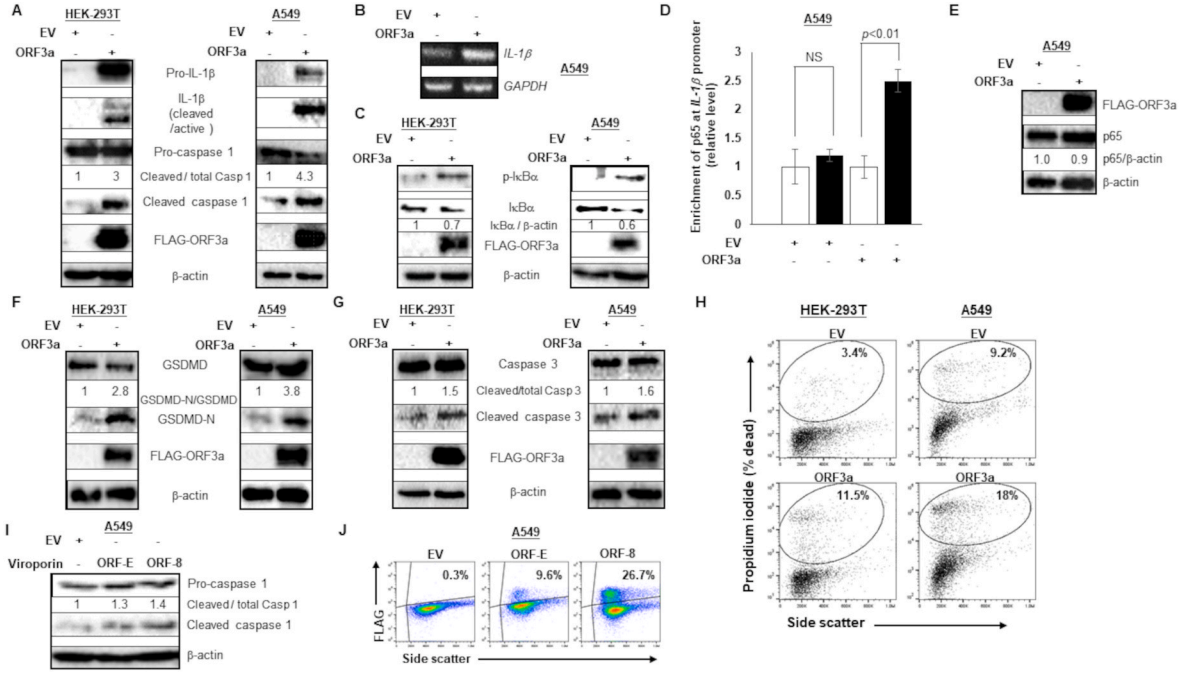

Fig. 1. ORF3a primes and activates the inflammasome, causing cell death. HEK-293T cells (A, C, F, G; left panels) or A549 cells (A, C, F, G; right panels) were transfected with FLAG-tagged ORF3a or empty vector (EV) and harvested after 24 h for immunoblotting with indicated antibodies. (B, D, E) ORF3a-transfected A549 cells were analyzed at 24 h by reverse transcriptase-PCR for *IL-1β* mRNA abundance (B), ChIP-PCR to quantify relative enrichment of NFκB p65 at the *IL-1β* promoter using anti-p65 antibodies (black bar) or control IgG (white bar) (D), or immunoblotting as indicated (E). (H) Unfixed cells harvested 24 h after transfection with EV or ORF3a were stained with propidium iodide (PI) followed by flow cytometry to enumerate percent dead cells. (I, J) FLAG-tagged ORF-E plasmid, ORF-8 plasmid, or EV was introduced into A549 cells. Cells were harvested 24 h later and subjected to immunoblotting (I) or flow cytometry using an anti-FLAG antibody (J); error bars in D, SEM of 3 independent experiments; NS, not significant. Experiments were performed three times.

the inflammasome, we found that it enhanced NLRP3 transcript and protein levels (Fig. 2A, upper panels showing NLRP3 protein and lower panel showing *NLRP3* transcript levels), and knockdown of NLRP3 curbed ORF3a protein-directed caspase 1 cleavage (Fig. 2B), indicating priming and activation of the NLRP3 inflammasome by ORF3a protein. Further, MCC950, a selective small molecule inhibitor that binds to the NACHT domain of NLRP3 and curtails its activation by blocking ATP hydrolysis (Coll et al., 2019), also blocks ORF3a protein-mediated activation of the inflammasome in low micromolar concentrations (Fig. 2C). Moreover, with the NIMA-related kinase NEK7 recently linked to NLRP3 activation (He et al., 2016), we also depleted NEK7 and found that ORF3a protein was impaired in its ability to cause cleavage of pro-caspase 1, i.e. unable to activate the inflammasome (Fig. 2D). The NLRP3 inflammasome is activated by a variety of cell-extrinsic and -intrinsic stimuli that trigger the assembly of the inflammasome machinery wherein NLRP3 oligomerizes with the adaptor protein ASC (Apoptosis-associated speck-like protein containing a CARD) leading to recruitment of pro-caspase 1 which is then activated by proximity-induced intermolecular cleavage. This cleavage of pro-caspase 1 is a central event in activation of the inflammasome. Given that ORF3a protein was able to activate the inflammasome in HEK-293T cells that lack ASC (as shown in Fig. 2E), we asked if ORF3a protein activated the inflammasome solely in an ASC-independent manner. We found that ORF3a protein's ability to activate pro-caspase 1 was substantially impaired upon depletion of ASC in A549 cells (Fig. 2F), supporting the idea that ORF3a protein activates the inflammasome in both ASC-dependent and -independent ways. To assess if ORF3a protein also activates other prominent inflammasomes NLRP1 and NLRC4, both able to recruit and activate pro-caspase 1 in ASC-dependent and -independent ways (Broz et al., 2010; Jin et al., 2013; Malik and Kanneganti, 2017), we depleted each of these molecules but were unable to block cleavage of pro-caspase 1 (Fig. 2G), indicating that ORF3a protein predominantly activates the NLRP3 inflammasome.

2.3. ORF3a protein triggers NLRP3 inflammasome assembly and activation via K^+ efflux

With NEK7 a key mediator of NLRP3 activation downstream of potassium efflux, and efflux of potassium ions a central mechanism of NLRP3 activation, particularly by ion channel-inducing viroporins (Chen et al., 2019; Farag et al., 2020; He et al., 2016), we investigated the effect of blocking potassium efflux by raising the extracellular concentration of K^+ and found that ORF3a protein-mediated caspase 1 cleavage was abrogated (Fig. 3A). To identify the type of K^+ channel formed by ORF3a protein, we employed known pharmacologic inhibitors including quinine, barium ($BaCl_2$), iberiotoxin, and tetraethylammonium (TEA) to block two-pore domain K^+ channels, inward-rectifier K^+ channels, large conductance calcium-activated K^+ channels, and voltage gated K^+ channels, respectively (Di et al., 2018). Mimicking the ability of barium to block the release of SARS-CoV virions (Lu et al., 2006) and supporting the finding in Fig. 3A, barium was able to curb SARS-CoV-2 ORF3a protein-mediated activation of caspase 1, indicating that ORF3a protein forms inward-rectifier K^+ channels in the membrane (Fig. 3B). Furthermore, using coimmunoprecipitation, we found that restricting K^+ efflux also impaired ORF3a protein's ability to trigger assembly of both ASC-independent (Fig. 3C; HEK-293T cells) and -dependent (Fig.3D; A549 cells) NLRP3 inflammasomes. Thus, ORF3a protein activates the NLRP3 inflammasome by causing K^+ efflux which then triggers NEK7-NLRP3 interaction leading to recruitment of ASC and pro-caspase 1.

2.4. SARS-CoV-2 activates the NLRP3 inflammasome via K^+ efflux

We next addressed if SARS-CoV-2 infection of epithelial cells also activated the NLRP3 inflammasome and if so, whether activation relied on K^+ efflux. Mirroring the experiments with transfected ORF3a protein, we found that infecting HEK-293T cells and A549 cells with SARS-CoV-2 increased the abundance of cleaved/active caspase 1 (Fig. 4A and B). Consistent with activation of the NLRP3 inflammasome, this process was sensitive to the NLRP3 inhibitor MCC950. Furthermore, also similar to experiments with ORF3a protein, SARS-CoV-2 infection in the presence of high levels of extracellular K^+ resulted in a drop in the abundance of

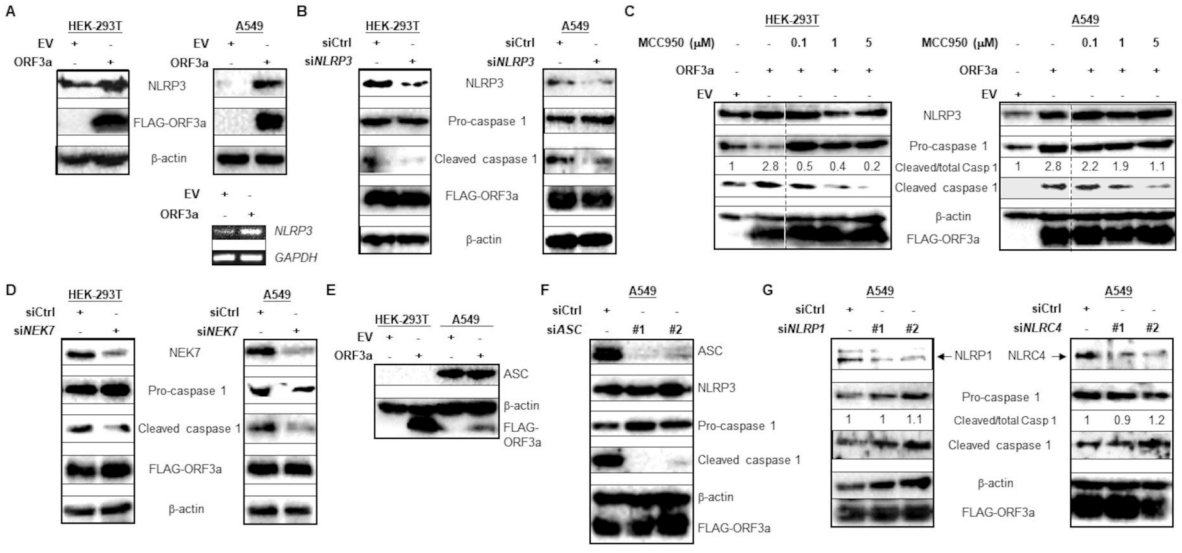

Fig. 2. ORF3a activates the NEK7-NLRP3 inflammasome via ASC-dependent and independent modes. (A) Lysates of FLAG-ORF3a- or empty vector (EV)-transfected HEK-293T (left) or A549 (right) cells were immunoblotted with indicated antibodies. In parallel, A549 cells transfected with FLAG-ORF3a or EV were examined for *NLRP3* transcripts using RT-PCR (panel beneath A549 immunoblot). (B, D) HEK-293T (left) or A549 (right) cells were co-transfected with FLAG- ORF3a and control siRNA (B, D), *NLRP3* siRNA (B), or *NEK7* siRNA (D) for 24 h prior to immunoblotting with indicated antibodies. (C) HEK-293T (left) or A549 (right) cells were transfected with EV or FLAG-ORF3a and exposed to MCC950 for 24 h prior to immunoblotting. (E) Lysates of cells transfected with ORF3a or EV were immunoblotted with indicated antibodies. (F, G) A549 cells were co-transfected with FLAG-ORF3a and control siRNA, *ASC* siRNA (F), *NLRP1* siRNA (G; left), or *NLRC4* siRNA (G, right) for 24 h prior to immunoblotting with indicated antibodies. Experiments were performed at least thrice.

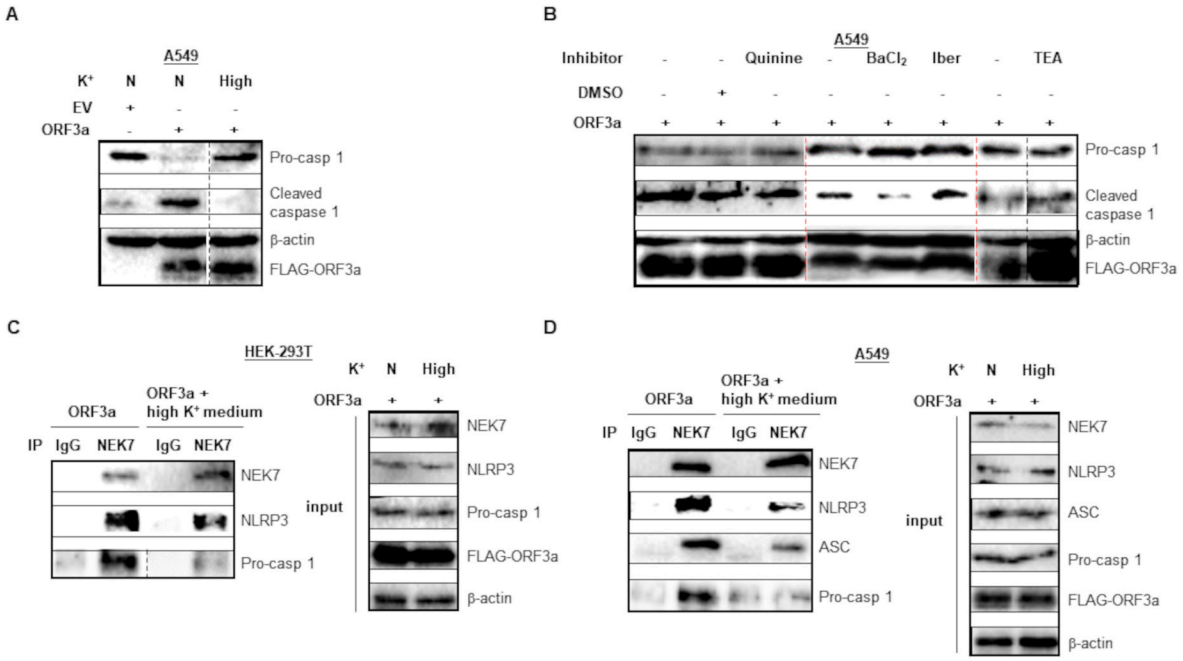

Fig. 3. ORF3a-mediated activation of NLRP3 inflammasome requires K^+ efflux. (A) FLAG-ORF3a plasmid or empty vector (EV) were introduced into A549 cells. After 20 h, cells were left in normal medium (N) or exposed to medium with high K^+ (50 mM; to block K^+ efflux; High). Cells were harvested 4 h later, and extracts immunoblotted with indicated antibodies. (B) A549 cells transfected with FLAG-ORF3a were exposed to indicated potassium channel inhibitors quinine, barium (BaCl2), iberiotoxin (Iber), and tetraethylammonium (TEA) for 2 h prior to immunoblotting with different antibodies; red lines demarcate experimental groups; black line indicates lanes from different regions of the same gel (−/+ TEA); lanes 1–3 and lanes 2–6 were run on two different gels. (C and D) FLAG-ORF3a plasmid was introduced into HEK-293T (C) and A549 (D) cells. After 20 h, cells were left in normal medium (N) or exposed to medium with high K^+ (High). Cells were harvested 4 h later, and extracts immunoblotted (Input) or immunoprecipitated with control IgG or anti-NEK7 antibody followed by immunoblotting with indicated antibodies. Input represents 5% of sample. Experiments were performed at least twice.

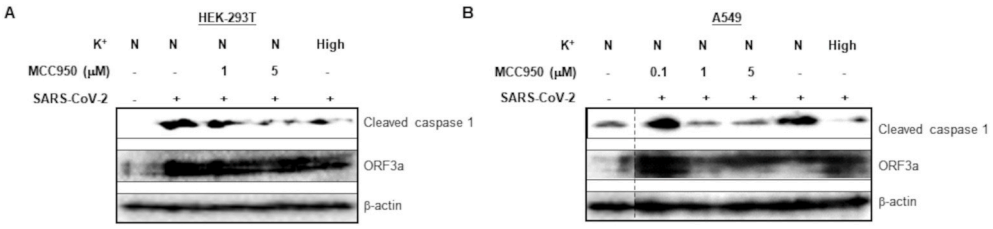

Fig. 4. Infection with SARS-CoV-2 causes activation of the NLRP3 inflammasome. HEK293T (A) and A549 (B) cells were infected with SARS-CoV-2 in the presence or absence of MCC950, normal (N) or high K^+ containing medium (High; for the last 20 h of culture), and harvested after 24 h for immunoblotting with indicated antibodies. Experiments were performed twice.

cleaved caspase 1 to near baseline levels, implicating K^+ efflux in SARS-CoV-2-triggered activation of the inflammasome. As expected, ORF3a protein was expressed in infected HEK-293T and A549 cells, though the abundance appeared to be lower in the presence of MCC950 in A549 cells (Fig. 4A and B). This apparent reduction in ORF3a levels could be due to technical reasons. Alternatively, inflammasome activation may provide positive feedforward activation of virus replication resulting in more ORF3a protein, which is disrupted in MCC950-treated cells. We recently discovered such a NLRP3-mediated feedforward positive activation of virus reactivation/replication for Epstein-Barr virus (Burton et al., 2020, 31919284). While this is possible in the case of ORF3a-mediated inflammasome activation, we favor the first possibility, i.e. a technical issue, because MCC950 did not negatively affect the levels of ORF3a protein in HEK-293T cells in Fig. 4A.

2.5. *FDA-approved drugs with anti-inflammatory properties block ORF3a-triggered activation of the NLRP3 inflammasome*

Understanding how ORF3a protein induces assembly and activation of the inflammasome, we next tested the ability of three orally available drugs that are in regular use in the clinic for their ability to block inflammasome activation. The oldest of the three, Doxycycline, is an antibiotic found to have anti-NLRP3 properties in mouse models of *Leptospira* and *P. gingivalis* (Xu et al., 2019b; Zhang et al., 2017). The second, Metformin, is an antidiabetic agent that suppressed NLRP3 in animal models of diabetic cardiomyopathy and psoriasis (Tsuji et al., 2020; Yang et al., 2019). The youngest, Ibrutinib, used to treat mantle cell lymphoma, was also found to block the NLRP3 inflammasome in an animal model of ischemic stroke (Ito et al., 2015; Liu et al., 2017). Using concentrations that were used in these publications, we tested the three drugs and found that all three impaired ORF3a protein's ability to activate the inflammasome, returning cleaved caspase 1 to near baseline levels (Fig. 5A–C). In addition, corroborating these findings, ORF3a protein-induced extracellular release of cleaved/mature IL-1β was blunted or obliterated by the three drugs, and as expected, by MCC950 (Fig. 5D); of note, HEK-293T cells also exhibited baseline levels of IL-1β release (Fig. 5D, left panel).

We also evaluated potential toxicity of the FDA-approved drugs and

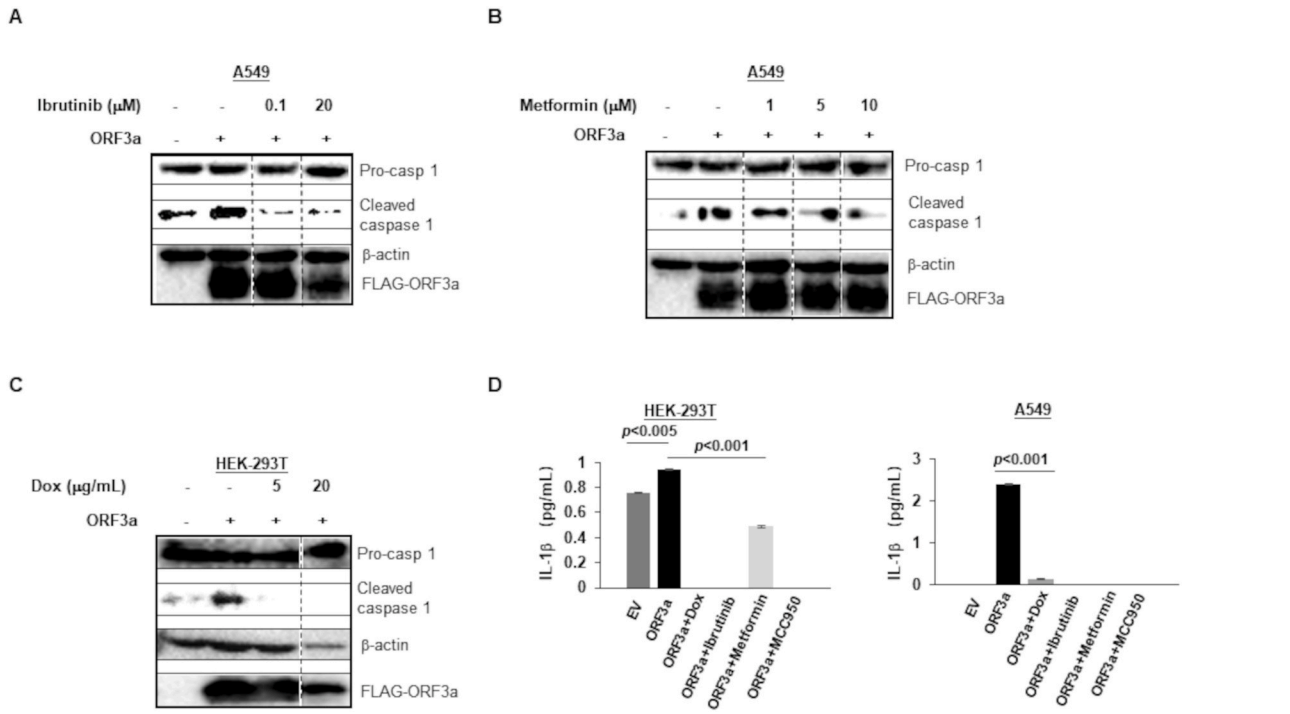

Fig. 5. ORF3a-mediated activation of NLRP3 inflammasome is inhibited by commonly used drugs. (A–C) A549 (A, B) and HEK293T (C) cells were transfected with ORF3a plasmid, exposed to Ibrutinib, Metformin, and Doxycycline at indicated concentrations for 24 h, and subjected to immunoblotting. (D) HEK293T (left) and A549 (right) cells were transfected with ORF3a plasmid, exposed to Doxycycline (5 μg/mL), Ibrutinib (1 μM), Metformin (10 μM), and MCC950 (5 μM) for 24 h, and IL-1β release in the culture supernatant was measured by ELISA. Experiments were performed at least twice.

other chemicals used in this study. We found that in concentrations used in HEK-293T and A549 cells in Figs. 2, 3 and 5, most of the drugs were not toxic. However, we observed a small but significant level of toxicity at both 5 and 20 μg/ml Doxycycline (Fig. 6A and B). Collectively, these experiments assert the importance of ion channels and NLRP3 in SARS-CoV-2-triggered activation of the inflammasome and highlight three FDA-approved drugs able to curtail this activation to variable degrees.

2.6. Key residues in ORF3a protein important for activating the inflammasome are well conserved

Alignment of ORF3a protein sequences from SARS-CoV-2 isolates from Asia, Europe, Middle-East, Russia, and North and South America as well as other bat CoVs and SARS-CoV revealed the conservation of two out of three key cysteine residues (residues 127, 130, and 133), shown to be essential for K^+ channel formation by SARS-CoV (Chen et al., 2019) (Fig. 7A). The exception, cysteine 127, was replaced by leucine in all SARS-CoV-2 isolates. We also observed a similar switch from cysteine to valine at position 121 and a switch from asparagine to cysteine at position 153 in all SARS-CoV-2 isolates. Introducing single point mutations at positions 127, 130, and 133 of SARS-CoV-2 ORF3a protein impaired its ability to activate the inflammasome, supporting the need for not only the two conserved cysteines at positions 130 and 133 but also that of the newly acquired leucine at position 127 of SARS-CoV-2 ORF3a protein (Fig. 7B, left panel). Similarly, mutating the residues at positions 121 and 153, both newly acquired in SARS-CoV-2 though conserved in all isolates, also resulted in a dampened response by the inflammasome (Fig. 7B, right panel). Thus, SARS-CoV-2 ORF3a protein has retained some of the key residues needed for virus release and inflammasome activation but has acquired additional changes that support a functionally consequential divergence from earlier CoVs. Nonetheless, this domain bearing the abovementioned residues that is essential for forming ion channels for virus release has remained remarkably well conserved throughout the pandemic, including the most infectious variants of concern such as the B.1.1.7, Delta, and Delta-Plus variants, thereby maintaining its ability to activate the inflammasome.

3. Discussion

In summary, a viroporin required for release of SARS-CoV-2 from

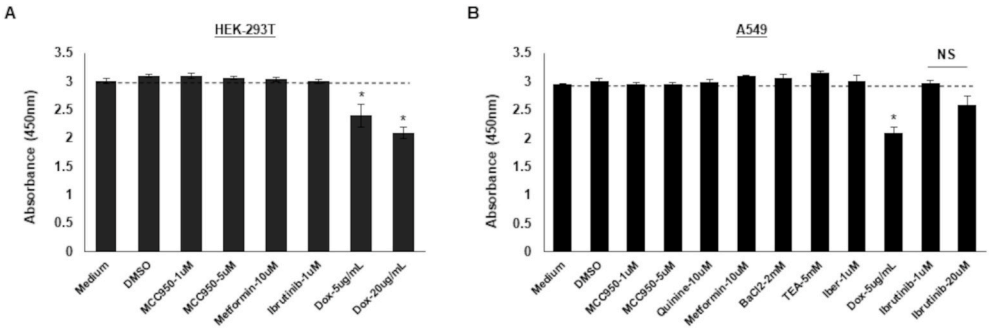

Fig. 6. Most drugs and chemicals used in this study demonstrate minimal to no toxicity. HEK-293 (A) and A549 (B) cells were left untreated (medium), exposed to DMSO, or treated with drugs/chemicals at indicated concentrations matching those in experiments depicted in Figs. 2, 3, and 5. Cells were harvested 24 h later for assessment of viability using the WST-1 assay. NS, not significant. Error bars show SEM of reads from triplicate wells; *, $p < 0.05$. The experiment was performed twice.

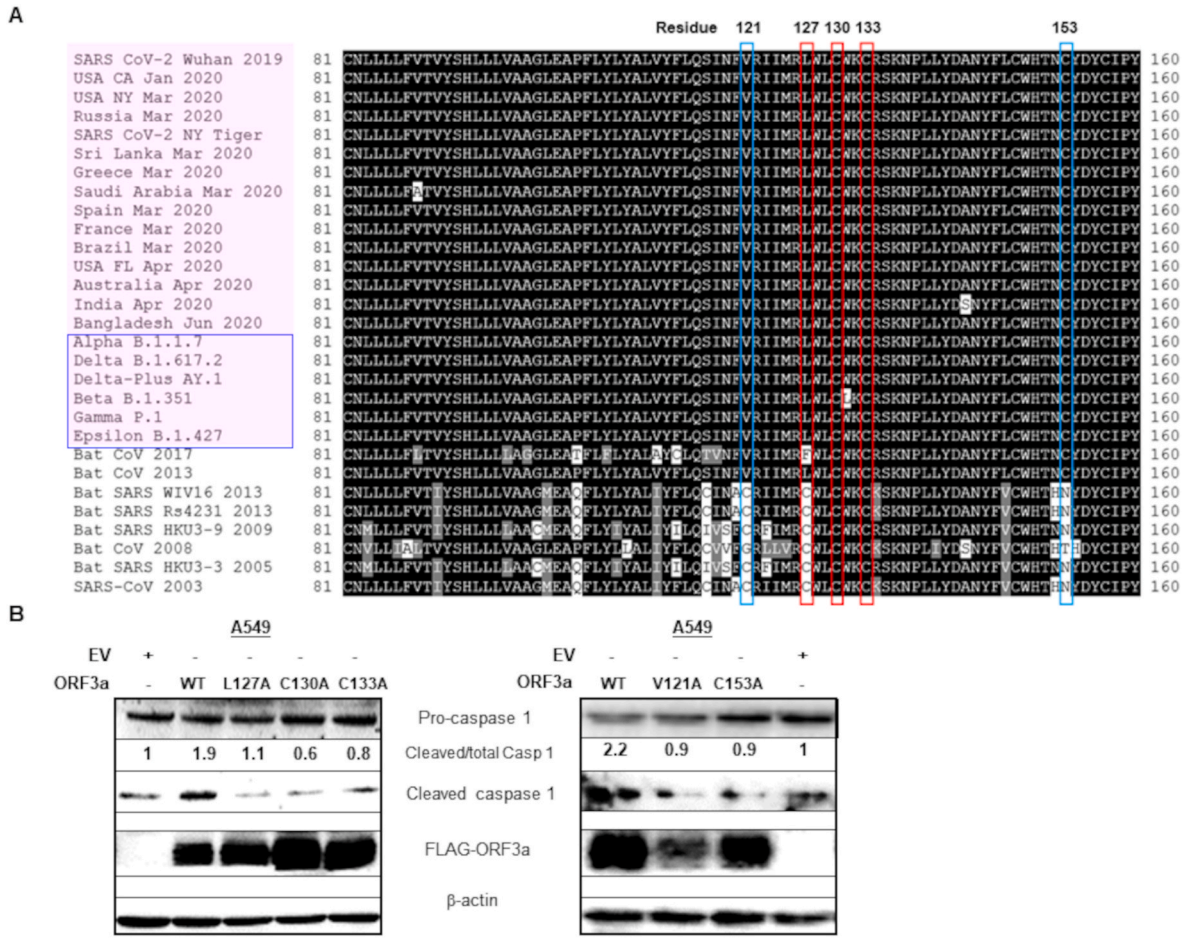

Fig. 7. ORF3a residues required for inflammasome activation are conserved in SARS-CoV-2 isolates across continents, including highly infectious variants of concern. (A) ORF3a/ORF3 viroporin from SARS-like betacoronaviruses including temporally and geographically distinct isolates from the COVID-19 pandemic and diverse species isolates dating back to the original SARS pandemic of 2003 were aligned in CLUSTAL Omega using EMBL-EBI Server Tools (https://www.ebi.ac.uk/Tools/services/web_clustalo/toolform.ebi). Selected isolates displaying the most diversity are shown from positions 81 to 160 of ORF3a/ORF3. SARS-CoV-2 isolates are shaded in pink with highly infectious variants of concern outlined in blue. Conserved cysteine residues previously identified in SARS-CoV as critical to K^+ ion channel formation are outlined in red. Newly divergent residues (121 and 153) conserved across SARS-CoV-2 isolates are outlined in blue. The multiple sequence alignment was shaded in BoxShade hosted by ExPASy (https://embnet.vital-it.ch/software/BOX_form.html). (B) A549 cells were transfected with EV, wild-type FLAG-ORF3a (WT), or FLAG-ORF3a mutants. Cells were harvested 24 h later and immunoblotted with indicated antibodies. Experiments were performed at least twice. (For interpretation of the references to colour in this figure legend, the reader is referred to the Web version of this article.)

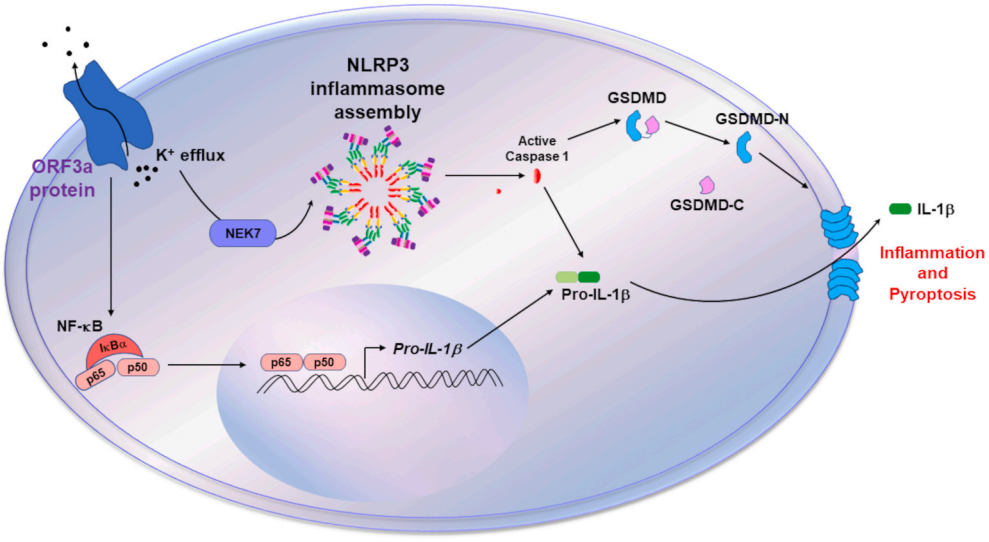

Fig. 8. Model of SARS-CoV-2 ORF3a protein-mediated activation of the NLRP3 inflammatory pathway. ORF3a protein primes the inflammasome via NF-κB-mediated transcriptional activation of pro-IL-1β. ORF3a protein also activates the NLRP3 inflammasome via K^+ efflux and NEK7. Assembly/activation of NLRP3 inflammasome activates caspase 1 which causes cleavage of pro-IL-1β into mature IL-1β as well as cleavage of GSDMD into its N- and C-terminal fragments. N-terminal GSDMD (GSDMD-N) forms non-selective pores at the cell membrane through which IL-1β is released resulting in inflammation and cell death by pyroptosis.

infected cells is also able to prime and activate the NLRP3 inflammasome, the machinery responsible for much of the inflammatory pathology in severely ill patients. Fig. 8 depicts a mechanistic model of SARS-CoV-2 ORF3a protein-mediated priming and activation of the NLRP3 inflammasome that results in release of the proinflammatory cytokine IL-1β and death of epithelial cells. ORF3a protein's importance to the virus's life cycle makes it an attractive therapeutic candidate. Moreover, while different from its homologs in other CoVs, the high conservation of the newly divergent SARS-CoV-2 ORF3a protein across isolates from several continents combined with our observation that multiple single point mutations reduce its ability to activate the inflammasome, argues against rapid emergence of resistance phenotypes. Thus, targeting ORF3a protein has the dual potential of blocking virus spread and inflammation.

Conserved and newly divergent amino acid residues in ORF3a protein contribute to forming K^+ channels that trigger NLRP3 activation. Notably, these residues have remained unchanged despite the evolution of SARS-CoV-2 over the last year, including the highly infectious Delta and Delta-Plus variants. This underscores the idea that targeting the NLRP3-ORF3a protein relationship may be important particularly as we face the possibility of a rapidly mutating virus able to escape vaccines and antiviral strategies that may target the virus. In that context, we have identified three candidate oral drugs that are used in the clinic for other purposes but may be re-purposed for COVID-19. Such mechanism-guided repurposing of drugs with which we already have extensive field experience in safety and tolerability, may provide a rapid path to clinical trials and emergency use authorization.

SARS-CoV-2 is not only linked to severe and fatal outcomes in adults with underlying comorbidities associated with pre-existing inflammation, it also causes severe disease in children in the form of Multisystem Inflammatory Syndrome in Children (MIS-C) as well as in adults as MIS-A (Feldstein et al., 2020; Morris et al., 2020). Dampening the inflammatory response in such patients is therefore an attractive strategy – a strategy that has shown promise in patients treated with Anakinra, a recombinant IL-1R antagonist (Cavalli et al., 2020; Huet et al., 2020). Notably, for several inflammatory diseases, there is keen interest within the pharmaceutical industry in therapeutically targeting the inflammatory pathway at a further upstream point, namely NLRP3 itself. MCC950 is a prototype of this approach with several other related compounds undergoing preclinical, phase I, and phase II trials (https://cen.acs.org/pharmaceuticals/drug-discovery/Could-an-NLRP3-inhibitor-be-the-one-drug-to-conquer-common-diseases/98/i7). Along the same lines, Gasdermin D, also activated by ORF3a protein, presents yet another therapeutic target as it may potentiate virus release by killing cells in addition to causing inflammation. Additionally, restraining the NLRP3 inflammasome may secondarily stifle virus replication itself as we recently demonstrated for a DNA tumor virus (Burton et al., 2020). That said, while our studies point towards a role for ORF3a protein in activation of the inflammasome, its relative contribution in infection studies remain to be elucidated. Indeed, other viroporins and other viral proteins may also contribute. Moreover, if and how ORF3a protein contributes to pathogenicity in animal models and humans is also presently unclear.

ORF3a protein of SARS-CoV has been shown to activate the NLRP3 inflammasome by promoting TRAF3-dependent ubiquitination of ASC (Siu et al., 2019). More recently, while our manuscript was under review, non-structural protein 6 of SARS-CoV-2 was found to activate the NLRP3 inflammasome by targeting a vacuolar ATPase proton pump component (Sun et al., 2022). Although SARS-CoV-2 ORF-E was also recently reported to enhance NLRP3 inflammasome, this occurred during the later stages of infection (Yalcinkaya et al., 2021). Two other studies using autopsy samples from deceased COVID-19 patients have demonstrated that the NLRP3 inflammasome is indeed strongly activated in lung alveolar epithelial cells (Rodrigues et al., 2021; Toldo et al., 2021), further underscoring the relevance of our findings. Activation of the NLRP3 inflammasome also bears mention in broader contexts. In particular, two reports have found that a fraction of severely ill COVID-19 patients display defective type I interferon immunity (Bastard et al., 2020; Zhang et al., 2020). It is likely that severe disease in these individuals also stemmed from unchecked pro-inflammatory responses since type I interferon can counteract the NLRP3 inflammasome in a number of ways (Labzin et al., 2016). Similarly, for those who have metabolic disturbances such as hypokalemia that often results from antihypertensive medications, ORF3a protein may have a lower threshold for activating the inflammasome due to a higher K^+ gradient across the infected cell.

4. Methods

4.1. Cell lines and infection

Human embryonic kidney-293T (HEK-293T) cells were maintained in DMEM (Thermo Fisher Scientific, Cat. 11965118) containing 10% fetal bovine serum (GEMINI, Cat. 900108) and 1% penicillin/streptomycin (Gibco, Cat. 15140122). A549 cells were maintained in Ham's F-12 Nutrient Mix (Thermo Fisher Scientific, Cat. 11765054) containing 10% fetal bovine serum and 1% penicillin/streptomycin. Both cell lines were cultured in the presence of 5% CO2 at 37 °C. Cells were infected in a BSL-3 lab with the UF-1 strain of SARS-CoV-2 at MOI of 4 in media containing 3% low IgG FBS (Fisher Scientific, Cat. SH30070.03).

4.2. Plasmids, siRNAs, and transfection

ORF3a, *ORF-E*, and *ORF-8* genes without stop codons (nt 25,382–26,206, nt 26,234–26,458 and nt 27,883-nt 28,245, GenBank accession no. MT295464.1) were PCR amplified with forward primer (5′CGCGGATCCATGGATTTGTTTATGAGAATCTT3′) and reverse primer (5′ AAGGAAAAAAGCGGCCGCCAAAGGCACGCTAGTAGTC3′), forward primer (5′ CGCGGATCCATGTACTCATTCGTTTCGG′) and reverse primer (5′ AAGGAAAAAAGCGGCCGCGACCAGAAGATCAGGAACT3′), forward primer (5′ CGCGGATCCATGAAATTTCTTGTTTTCTTAGGA′) and reverse primer (5′ AAGGAAAAAAGCGGCCGCGATGAAATCTAAAACAACACGAA 3′), respectively, by using Phusion High-Fidelity DNA Polymerase (New England Biolabs, M0530L) according to the manufacturer's protocol and inserted into pcDNA5.1/FRT/TO vector (a kind gift from professor Torben Heick Jensen, Denmark) with a C-terminal 3 × FLAG tag to generate FLAG-tagged ORF3a plasmid. Flag-tagged ORF3a mutants (V121A, L127A, C130A, C133A, C153A) were constructed by overlap extension PCR with the following primer pairs:

5′GAGTATAAACTTTGCAAGAATAATAATGAG3' (forward) and 5′CTCATTATTATTCTTGCAAAGTTTATACTC3' (reverse), 5′ATAATG AGGGCTTGGCTTTG3' (forward) and 5′CAAAGCCAAGCCCTCATTAT3' (reverse), 5′GCTTTGGCTTGCCTGGAAATGC3' (forward) and.

5′GCATTTCCAGGCAAGCCAAAGC3' (reverse),

5′TGCTGGAAAGCCCGTTCCAAA3' (forward) and.

5′TTTGGAACGGGCTTTCCAGCA3' (reverse), 5′GCATACTAATG CTTACGACTATTG3' (forward) and 5′CAATAGTCGTAAGCATTAGT ATGC3' (reverse), respectively.

HEK-293T and A549 cells were transfected with LipoJet™ In Vitro Transfection Kit (SignaGen Laboratories, SL100468) according to the manufacturer's protocol.

HEK-293T and A549 cells were transfected with 200 pmoles of siRNA. siRNAs included *NLRP3* (Ambion, Cat. s41554), *NEK7* (Ambion, Cat. 103794), *ASC* (Ambion, Cat. 44232 and 289672), *NLRP1* (#1, Ambion, Cat. S22520; #2, Ambion, Cat. 239345), *NLRC4* ((#1, Ambion, Cat. S33828; #2, Ambion, Cat. 105219), and control (Dharmacon, Cat. D001810-01-20).

4.3. SARS-CoV-2

A passage two stock of *Severe acute respiratory syndrome coronavirus 2* isolate SARS-CoV-2/human/USA/UF-1/2020 (GenBank MT295464)

was used for virus-infection studies. The virus was the first isolate from a patient at the University of Florida Health Shands Hospital (J. Lednicky, unpublished) and has about 99% nt identity with SARS-CoV-2 reference strain Wuhan-Hu-1 (GenBank NC_045512.2) and 100% identity with the genomes of SARS-CoV-2 detected in California, USA. The genome of SARS-CoV-2 UF-1 encodes an aspartic acid residue at amino acid 614 of the spike protein. This virus was isolated and then propagated (one passage) in VeroE6 cells prior to sequence analyses and use in this work, and has no INDELs in its genome. All work with this virus was performed in a BSL-3 laboratory by an analyst using a full-head powered-air purifying respirator and appropriate personal protective equipment, including gloves and a chemically impervious Tyvek gown.

4.4. Chemical treatment of cell lines

HEK-293T and A549 cells were transfected with plasmids. After 2h, different chemical reagents were added to medium. Chemical reagents included NLRP3 inhibitor MCC950 (0.1–5 μM) (Sigma Aldrich, Cat. 538120), Quinine (10 μM) (Sigma Aldrich, Cat. 145904), Barium chloride (2 mM) (Sigma Aldrich, Cat. 342920), Tetraethylammonium chloride (5 mM) (Tocris Bioscience, Cat. 306850), Iberiotoxin (1.0 μM) (Tocris Bioscience, Cat. 1086100U), Doxycycline (Sigma Aldrich, Cat. D3447), Ibrutinib (R&D, Cat. 6813), and Metformin (R&D, Cat. 2864). All chemicals were dissolved with DMSO or sterile water.

4.5. Reverse transcription PCR (RT-PCR)

RT-PCR was performed as previously described (King et al., 2015). Briefly, 1 μg of total RNA was used as template for complementary DNA synthesis using MuLV reverse transcriptase (New England Biolabs, Cat. M0253L) according to the manufacture's protocol. OneTaq DNA Polymerase (New England Biolabs, Cat. M0480S) was used to amplify DNA fragment using manufacture's protocol. RT-PCR primers were as following:

forward primer 5′ACCATCTTCCAGGAGCGAGA3′ and
reverse primer 5′GGCCATCCACAGTCTTCTGG 3′ for *GAPDH* mRNA,
forward primer 5′TCAGCCAATCTTCATTGCTC3′ and
reverse primer 5′GCCATCAGCTTCAAAGAACA3′ for *IL-1β* pre-mRNA (Siu et al., 2019),
forward primer 5′CGAATCCCACTGTGATATGCC3′ and
reverse primer 5′GTGTGTAGCGTTTGTTGAGGC3′ for *NLRP3* mRNA.

4.6. Immunoblotting and antibodies

Immunoblotting was performed as previously described (Burton et al., 2020). Briefly, total cell lysates were electrophoresed on 10% or 12% SDS-polyacrylamide gels and transferred onto nitrocellulose membranes and immunoassayed with indicated antibodies. The following antibodies were used: rabbit anti-Caspase-1 antibody (Thermo Scientific, Cat. PA587536), rabbit anti-cleaved Caspase-1 antibody (Thermo Scientific, Cat. PA538099), mouse anti-IL-1β (Cell Signaling Technology, Cat. 12242s), mouse anti-Flag M2 antibody (Sigma-Aldrich, Cat. F1804), mouse anti-β-actin antibody (Sigma-Aldrich, Cat. A5441), rabbit anti-phospho-IκBα (Ser32) antibody (Cell Signaling Technology, Cat. 2859s), rabbit anti-IκBα antibody (Cell Signaling Technology, Cat. 9242s), rabbit anti–NF–κB p65 antibody (Cell Signaling Technology, Cat. 8242s), rabbit anti-Caspase 3 antibody (GeneTex, Cat. GTX110543), rabbit anti-Gasdermin D (L60) antibody (Cell Signaling Technology, Cat. 93709s), rabbit anti-cleaved-Gasdermin D (Asp275) antibody (Cell Signaling Technology, Cat. 36425s), rabbit anti-NLRP3 antibody (Invitrogen, Cat. PA5-21745), rabbit anti-NEK7 antibody (Cell Signaling Technology, Cat. 3057s), rabbit anti-ASC antibody (Cell Signaling Technology, Cat. 13833s), rabbit anti-NLRP1 antibody (Novus Biologicals, Cat. NB100–56147SS), rabbit anti-NLRC4 antibody (Novus Biologicals, Cat. NB100–56142SS), rabbit anti-SARS-CoV-2 ORF3a antibody (FabGennix, Cat. SARS-COV2-ORF3A-101AP), HRP-conjugated goat anti-mouse IgG (H + L) (Thermo Scientific, Cat. 626520) and HRP conjugated goat anti-rabbit IgG(H + L) (Thermo Scientific, Cat. 31460), and HRP conjugated goat anti-rabbit IgG (light chain) (Novus, Cat. NBP2-75935).

4.7. Flow cytometry

Flow cytometry was performed as previous described (Xu et al., 2019a). Briefly, HEK-293T and A549 cells were transfected with EV, FLAG-ORF3a, FLAG-ORF-E, or FLAG-ORF-8. After 24 h, cells were treated with trypsin for 3 min and collected by centrifugation at 350*g* for 3 min. For cell death testing, cell pellets were washed twice with FACS buffer (1X PBS with 2% FBS) and resuspended in 200 μl of RNase-containing FACS buffer. 20 μl of propidium iodide (10 μg/ml) (Sigma-Aldrich, Cat. P4864) was added to each sample and subjected to flow cytometry immediately to assay cell death. For testing the expression of ORF-E and ORF-8 proteins, cells were fixed and permeabilized with cytofix/cytoperm solution (BD Bioscience, Cat. 554722) and incubated with mouse anti-FLAG antibody (Sigma-Aldrich, Cat. F1804) for 1 h. After washing with wash buffer, cells were incubated with FITC-conjugated goat anti-mouse IgG (Sigma-Aldrich, Cat. F0257) antibody prior to performing flow cytometry.

4.8. Chromatin immunoprecipitation-quantitative PCR (ChIP-qPCR)

ChIP was performed as described previously (Li et al., 2018). Briefly, A549 cells were transfected with FLAG-ORF3a or empty vector as control. Twenty-four hours later, cells (7.5×10^5 cells for each ChIP) were crosslinked with 1% formaldehyde for 20 min and quenched with 0.125 M glycine. Cells were lysed in 500 μl of nuclear extraction buffer A (Cell Signaling Technology, Cat. 7006) on ice for 15 min and washed once with 500 μl of nuclear extraction buffer B (Cell Signaling Technology, Cat. 7007), and then treated with 0.5 μL of micrococcal nuclease (Cell Signaling Technology, Cat. 10011) for 20 min at 37 °C. Nuclei were resuspended in 1 × ChIP buffer (Cell Signaling Technology, Cat. 7008) and sonicated at 8W with 10-s on and 20-s off pulses on ice for two cycles to break nuclear membranes. After removing debris, 2% of each sample was set aside as input and the rest (98%) of the sample was incubated with 3 μg of antibody (or 3 μg of IgG as control) and 30 μl of protein G magnetic beads (Cell Signaling Technology, Cat. 7008) at 4 °C overnight. Beads were washed three times with low salt ChIP buffer and once with high salt ChIP buffer. The protein-DNA complex were eluted with 1 × Elution buffer (Cell Signaling Technology, Cat. 10009). DNA was extracted with DNA purification columns (Cell Signaling Technology, Cat. 10010) and subjected to qPCR analysis. The following primers were used for amplifying the *IL-1β* promoter:

forward primer 5′AGGAGTAGCAAACTATGACAC3′ and
reverse primer 5′ACGTGGGAAAATCCAGTATTT3' (Hiscott et al., 1993).

4.9. Co-Immunoprecipitation (Co-IP)

Co-IP was performed as described previously (Li et al., 2017). Cells were lysed in ice-cold IP Lysis Buffer (Thermo Scientific, Cat. 87787) in the presence of 1 × protease inhibitor cocktail (Cell Signaling, #7012) for 15min followed by centrifugation (14,000 rpm) at 4 °C for 5 min. Of pre-cleared cell lysates, 5% was set aside as input. The rest was incubated with 3.0 μg of rabbit anti-NEK7 antibody (Bethyl Laboratories, Cat. A302-684A) or the same amount of control IgG (R&D, Cat. AB-105-C) together with 40 μl of Dynabeads Protein G (Thermo Scientific, Cat. 10003D) at 4 °C overnight. Beads were washed three times with IP lysis buffer and subjected to immunoblotting.

4.10. Enzyme-linked immunosorbent assay (ELISA)

ELISA was performed with Human IL-1β ELISA kit (R&D systems,

DLB50) following manufacturer's instructions. Briefly, cell free supernatant and serially diluted standard were incubated with antibody precoated wells for 2 h at room temperature. After three washes, 200 μL of conjugate was incubated for 1 h at room temperature followed by three more washes. Wells were then incubated with 200 μL of substrate for 20 min in the dark followed by addition of 50 μL of stop solution. Absorption was read at 450 nm using a microplate reader and quantitation performed using a standard curve.

4.11. Cell viability/toxicity assay

To check toxicity of drugs and other chemicals, a water-soluble tetrazolium salt (WST-1) assay was performed as described previously (Li et al., 2020). Briefly, 4×10^3 HEK-293T cells/well and 1×10^3 A549 cells/well were seeded into 96-well tissue culture microplates and cultured for 24 h followed by treatment of triplicate wells with drugs/chemicals for another 24 h. Then, 10 μL of WST-1 substrate (Sigma, Cat. 5015944001) was added per well and incubated at 37 °C for 2 h, and absorbance was measured at 450 nm using an ELISA reader.

4.12. Statistical analysis

Unpaired Student's *t*-test was used to calculate *p* values by comparing the means of two groups.

Funding

This research was conducted with funding from the Children's Miracle Network and the University of Florida (S.B.-M.).

Data and materials availability

All data is available in the main text.

CRediT authorship contribution statement

Huanzhou Xu: Conceptualization, Investigation, Formal analysis. **Ibukun A. Akinyemi:** Investigation. **Siddhi A. Chitre:** Investigation. **Julia C. Loeb:** Investigation. **John A. Lednicky:** Investigation. **Michael T. McIntosh:** Conceptualization, Investigation, Formal analysis, Supervision, Writing – review & editing. **Sumita Bhaduri-McIntosh:** Conceptualization, Formal analysis, Resources, Writing – original draft, Writing – review & editing, Supervision, Project administration, Funding acquisition.

Declaration of competing interest

The authors declare that they have no known competing financial interests or personal relationships that could have appeared to influence the work reported in this paper.

References

Ahn, M., Anderson, D.E., Zhang, Q., Tan, C.W., Lim, B.L., Luko, K., Wen, M., Chia, W.N., Mani, S., Wang, L.C., Ng, J.H.J., Sobota, R.M., Dutertre, C.A., Ginhoux, F., Shi, Z.L., Irving, A.T., Wang, L.F., 2019. Dampened NLRP3-mediated inflammation in bats and implications for a special viral reservoir host. Nat. Microbiol. 4, 789–799.

Baric, R.S., 2020. Emergence of a highly fit SARS-CoV-2 variant. N. Engl. J. Med. 383, 2684–2686.

Bastard, P., Rosen, L.B., Zhang, Q., Michailidis, E., Hoffmann, H.H., Zhang, Y., Dorgham, K., Philippot, Q., Rosain, J., Beziat, V., Manry, J., Shaw, E., Haljasmagi, L., Peterson, P., Lorenzo, L., Bizien, L., Trouillet-Assant, S., Dobbs, K., de Jesus, A.A., Belot, A., Kallaste, A., Catherinot, E., Tandjaoui-Lambiotte, Y., Le Pen, J., Kerner, G., Bigio, B., Seeleuthner, Y., Yang, R., Bolze, A., Spaan, A.N., Delmonte, O.M., Abers, M.S., Aiuti, A., Casari, G., Lampasona, V., Piemonti, L., Ciceri, F., Bilguvar, K., Lifton, R.P., Vasse, M., Smadja, D.M., Migaud, M., Hadjadj, J., Terrier, B., Duffy, D., Quintana-Murci, L., van de Beek, D., Roussel, L., Vinh, D.C., Tangye, S.G., Haerynck, F., Dalmau, D., Martinez-Picado, J., Brodin, P., Nussenzweig, M.C., Boisson-Dupuis, S., Rodriguez-Gallego, C., Vogt, G., Mogensen, T.H., Oler, A.J., Gu, J., Burbelo, P.D., Cohen, J., Biondi, A., Bettini, L.R., D'Angio, M., Bonfanti, P., Rossignol, P., Mayaux, J., Rieux-Laucat, F., Husebye, E.S., Fusco, F., Ursini, M.V., Imberti, L., Sottini, A., Paghera, S., Quiros-Roldan, E., Rossi, C., Castagnoli, R., Montagna, D., Licari, A., Marseglia, G.L., Duval, X., Ghosn, J., Lab, H., , Group, N.-U. I.R.t.C., Clinicians, C., Clinicians, C.-S., Imagine, C.G., French, C.C.S.G., Milieu Interieur, C., Co, V.C.C., , Amsterdam, U.M.C.C.-B., Effort, C.H.G., Tsang, J.S., Goldbach-Mansky, R., Kisand, K., Lionakis, M.S., Puel, A., Zhang, S.Y., Holland, S.M., Gorochov, G., Jouanguy, E., Rice, C.M., Cobat, A., Notarangelo, L.D., Abel, L., Su, H. C., Casanova, J.L., 2020. Auto-antibodies against type I IFNs in patients with life-threatening COVID-19. Science.

Broz, P., Dixit, V.M., 2016. Inflammasomes: mechanism of assembly, regulation and signalling. Nat. Rev. Immunol. 16, 407–420.

Broz, P., von Moltke, J., Jones, J.W., Vance, R.E., Monack, D.M., 2010. Differential requirement for Caspase-1 autoproteolysis in pathogen-induced cell death and cytokine processing. Cell Host Microbe 8, 471–483.

Burton, E.M., Goldbach-Mansky, R., Bhaduri-McIntosh, S., 2020. A promiscuous inflammasome sparks replication of a common tumor virus. Proc. Natl. Acad. Sci. U. S. A. 117, 1722–1730.

Cavalli, G., De Luca, G., Campochiaro, C., Della-Torre, E., Ripa, M., Canetti, D., Oltolini, C., Castiglioni, B., Din, C., Boffini, N., Tomelleri, A., Farina, N., Ruggeri, A., Rovere-Querini, P., DiLucca, G., Marinenghi, S., Scotti, R., Tresoldi, M., Ciceri, F., Zangrillo, A., Scarpellini, P., Dagna, L., 2020. Interleukin-1 blockade with high-dose anakinra in patients with COVID-19, acute respiratory distress syndrome, and hyperinflammation: a retrospective cohort study. Lancet Rheumatol.

Chen, I.Y., Moriyama, M., Chang, M.F., Ichinohe, T., 2019. Severe acute respiratory syndrome coronavirus viroporin 3a activates the NLRP3 inflammasome. Front. Microbiol. 10, 50.

Chen, W., Zhao, M., Zhao, S., Lu, Q., Ni, L., Zou, C., Lu, L., Xu, X., Guan, H., Zheng, Z., Qiu, Q., 2017. Activation of the TXNIP/NLRP3 inflammasome pathway contributes to inflammation in diabetic retinopathy: a novel inhibitory effect of minocycline. Inflamm. Res. 66, 157–166.

Coll, R.C., Hill, J.R., Day, C.J., Zamoshnikova, A., Boucher, D., Massey, N.L., Chitty, J.L., Fraser, J.A., Jennings, M.P., Robertson, A.A.B., Schroder, K., 2019. MCC950 directly targets the NLRP3 ATP-hydrolysis motif for inflammasome inhibition. Nat. Chem. Biol. 15, 556–559.

de Rivero Vaccari, J.C., Dietrich, W.D., Keane, R.W., de Rivero Vaccari, J.P., 2020. The inflammasome in times of COVID-19. Front. Immunol. 11, 583373.

Di, A., Xiong, S., Ye, Z., Malireddi, R.K.S., Kometani, S., Zhong, M., Mittal, M., Hong, Z., Kanneganti, T.D., Rehman, J., Malik, A.B., 2018. The TWIK2 potassium efflux channel in macrophages mediates NLRP3 inflammasome-induced inflammation. Immunity 49, 56–65 e54.

Dixit, V.D., 2013. Nlrp3 inflammasome activation in type 2 diabetes: is it clinically relevant? Diabetes 62, 22–24.

Farag, N.S., Breitinger, U., Breitinger, H.G., El Azizi, M.A., 2020. Viroporins and inflammasomes: a key to understand virus-induced inflammation. Int. J. Biochem. Cell Biol. 122, 105738.

Feldstein, L.R., Rose, E.B., Horwitz, S.M., Collins, J.P., Newhams, M.M., Son, M.B.F., Newburger, J.W., Kleinman, L.C., Heidemann, S.M., Martin, A.A., Singh, A.R., Li, S., Tarquinio, K.M., Jaggi, P., Oster, M.E., Zackai, S.P., Gillen, J., Ratner, A.J., Walsh, R. F., Fitzgerald, J.C., Keenaghan, M.A., Alharash, H., Doymaz, S., Clouser, K.N., Giuliano Jr., J.S., Gupta, A., Parker, R.M., Maddux, A.B., Havalad, V., Ramsingh, S., Bukulmez, H., Bradford, T.T., Smith, L.S., Tenforde, M.W., Carroll, C.L., Riggs, B.J., Gertz, S.J., Daube, A., Lansell, A., Coronado Munoz, A., Hobbs, C.V., Marohn, K.L., Halasa, N.B., Patel, M.M., Randolph, A.G., Overcoming, C.-I., the, C.D.C.C.-R.T., 2020. Multisystem inflammatory syndrome in U.S. Children and adolescents. N. Engl. J. Med. 383, 334–346.

Freeman, T.L., Swartz, T.H., 2020. Targeting the NLRP3 inflammasome in severe COVID-19. Front. Immunol. 11, 1518.

Grant, R.W., Dixit, V.D., 2013. Mechanisms of disease: inflammasome activation and the development of type 2 diabetes. Front. Immunol. 4, 50.

He, Y., Zeng, M.Y., Yang, D., Motro, B., Nunez, G., 2016. NEK7 is an essential mediator of NLRP3 activation downstream of potassium efflux. Nature 530, 354–357.

Hiscott, J., Marois, J., Garoufalis, J., D'Addario, M., Roulston, A., Kwan, I., Pepin, N., Lacoste, J., Nguyen, H., Bensi, G., et al., 1993. Characterization of a functional NF-kappa B site in the human interleukin 1 beta promoter: evidence for a positive autoregulatory loop. Mol. Cell Biol. 13, 6231–6240.

Hoffmann, M., Kleine-Weber, H., Schroeder, S., Kruger, N., Herrler, T., Erichsen, S., Schiergens, T.S., Herrler, G., Wu, N.H., Nitsche, A., Muller, M.A., Drosten, C., Pohlmann, S., 2020. SARS-CoV-2 cell entry depends on ACE2 and TMPRSS2 and is blocked by a clinically proven protease inhibitor. Cell 181, 271-280 e278.

Huet, T., Beaussier, H., Voisin, O., Jouveshomme, S., Dauriat, G., Lazareth, I., Sacco, E., Naccache, J.M., Bezie, Y., Laplanche, S., Le Berre, A., Le Pavec, J., Salmeron, S., Emmerich, J., Mourad, J.J., Chatellier, G., Hayem, G., 2020. Anakinra for severe forms of COVID-19: a cohort study. Lancet Rheumatol. 2, e393–e400.

Ito, M., Shichita, T., Okada, M., Komine, R., Noguchi, Y., Yoshimura, A., Morita, R., 2015. Bruton's tyrosine kinase is essential for NLRP3 inflammasome activation and contributes to ischaemic brain injury. Nat. Commun. 6, 7360.

Jin, T., Curry, J., Smith, P., Jiang, J., Xiao, T.S., 2013. Structure of the NLRP1 caspase recruitment domain suggests potential mechanisms for its association with procaspase-1. Proteins 81, 1266–1270.

Jin, Y., Fu, J., 2019. Novel insights into the NLRP 3 inflammasome in atherosclerosis. J. Am. Heart Assoc. 8, e012219.

King, C.A., Li, X., Barbachano-Guerrero, A., Bhaduri-McIntosh, S., 2015. STAT3 regulates lytic activation of kaposi's sarcoma-associated herpesvirus. J. Virol. 89, 11347–11355.

Labzin, L.I., Lauterbach, M.A., Latz, E., 2016. Interferons and inflammasomes: cooperation and counterregulation in disease. J. Allergy Clin. Immunol. 138, 37–46.

Li, X., Akinyemi, I.A., You, J.K., Rezaei, M.A., Li, C., McIntosh, M.T., Del Poeta, M., Bhaduri-McIntosh, S., 2020. A mechanism-based targeted screen to identify epstein-barr virus-directed antiviral agents. J. Virol. 94.
Li, X., Burton, E.M., Bhaduri-McIntosh, S., 2017. Chloroquine triggers Epstein-Barr virus replication through phosphorylation of KAP1/TRIM28 in Burkitt lymphoma cells. PLoS Pathog. 13, e1006249.
Li, X., Burton, E.M., Koganti, S., Zhi, J., Doyle, F., Tenenbaum, S.A., Horn, B., Bhaduri-McIntosh, S., 2018. KRAB-ZFP repressors enforce quiescence of oncogenic human herpesviruses. J. Virol. 92.
Liu, X., Pichulik, T., Wolz, O.O., Dang, T.M., Stutz, A., Dillen, C., Delmiro Garcia, M., Kraus, H., Dickhofer, S., Daiber, E., Munzenmayer, L., Wahl, S., Rieber, N., Kummerle-Deschner, J., Yazdi, A., Franz-Wachtel, M., Macek, B., Radsak, M., Vogel, S., Schulte, B., Walz, J.S., Hartl, D., Latz, E., Stilgenbauer, S., Grimbacher, B., Miller, L., Brunner, C., Wolz, C., Weber, A.N.R., 2017. Human NACHT, LRR, and PYD domain-containing protein 3 (NLRP3) inflammasome activity is regulated by and potentially targetable through Bruton tyrosine kinase. J. Allergy Clin. Immunol. 140, 1054–1067 e1010.
Liu, Y., Yan, L.M., Wan, L., Xiang, T.X., Le, A., Liu, J.M., Peiris, M., Poon, L.L.M., Zhang, W., 2020. Viral dynamics in mild and severe cases of COVID-19. Lancet Infect. Dis.
Lu, W., Zheng, B.J., Xu, K., Schwarz, W., Du, L., Wong, C.K., Chen, J., Duan, S., Deubel, V., Sun, B., 2006. Severe acute respiratory syndrome-associated coronavirus 3a protein forms an ion channel and modulates virus release. Proc. Natl. Acad. Sci. U. S. A. 103, 12540–12545.
Malik, A., Kanneganti, T.D., 2017. Inflammasome activation and assembly at a glance. J. Cell Sci. 130, 3955–3963.
Mehta, P., McAuley, D.F., Brown, M., Sanchez, E., Tattersall, R.S., Manson, J.J., Hlh Across Speciality Collaboration, U.K., 2020. COVID-19: consider cytokine storm syndromes and immunosuppression. Lancet 395, 1033–1034.
Moore, J.P., Offit, P.A., 2021. SARS-CoV-2 vaccines and the growing threat of viral variants. JAMA.
Morris, S.B., Schartz, N.G., Patel, P., Abbo, L., Beauchamps, L., Balan, S., Lee, E.H., 2020. Case series of Multisystem inflammatory syndrome in adults associated with SARS-CoV-2 infection - United Kingdom and United States, march-august 2020. Morb. Mortal. Wkly. Rep. 69, 1450–1456.
Nieto-Torres, J.L., DeDiego, M.L., Verdia-Baguena, C., Jimenez-Guardeno, J.M., Regla-Nava, J.A., Fernandez-Delgado, R., Castano-Rodriguez, C., Alcaraz, A., Torres, J., Aguilella, V.M., Enjuanes, L., 2014. Severe acute respiratory syndrome coronavirus envelope protein ion channel activity promotes virus fitness and pathogenesis. PLoS Pathog. 10, e1004077.
Nieto-Torres, J.L., Verdia-Baguena, C., Jimenez-Guardeno, J.M., Regla-Nava, J.A., Castano-Rodriguez, C., Fernandez-Delgado, R., Torres, J., Aguilella, V.M., Enjuanes, L., 2015. Severe acute respiratory syndrome coronavirus E protein transports calcium ions and activates the NLRP3 inflammasome. Virology 485, 330–339.
Nieva, J.L., Madan, V., Carrasco, L., 2012. Viroporins: structure and biological functions. Nat. Rev. Microbiol. 10, 563–574.
Puelles, V.G., Lutgehetmann, M., Lindenmeyer, M.T., Sperhake, J.P., Wong, M.N., Allweiss, L., Chilla, S., Heinemann, A., Wanner, N., Liu, S., Braun, F., Lu, S., Pfefferle, S., Schroder, A.S., Edler, C., Gross, O., Glatzel, M., Wichmann, D., Wiech, T., Kluge, S., Pueschel, K., Aepfelbacher, M., Huber, T.B., 2020. Multiorgan and renal tropism of SARS-CoV-2. N. Engl. J. Med. 383, 590–592.
Ratajczak, M.Z., Bujko, K., Ciechanowicz, A., Sielatycka, K., Cymer, M., Marlicz, W., Kucia, M., 2020. SARS-CoV-2 entry receptor ACE2 is expressed on very small CD45 (-) precursors of hematopoietic and endothelial cells and in response to virus spike protein activates the Nlrp3 inflammasome. Stem Cell Rev. Rep.
Rheinheimer, J., de Souza, B.M., Cardoso, N.S., Bauer, A.C., Crispim, D., 2017. Current role of the NLRP3 inflammasome on obesity and insulin resistance: a systematic review. Metabolism 74, 1–9.
Richardson, S., Hirsch, J.S., Narasimhan, M., Crawford, J.M., McGinn, T., Davidson, K. W., the Northwell, C.-R.C., Barnaby, D.P., Becker, L.B., Chelico, J.D., Cohen, S.L., Cookingham, J., Coppa, K., Diefenbach, M.A., Dominello, A.J., Duer-Hefele, J., Falzon, L., Gitlin, J., Hajizadeh, N., Harvin, T.G., Hirschwerk, D.A., Kim, E.J., Kozel, Z.M., Marrast, L.M., Mogavero, J.N., Osorio, G.A., Qiu, M., Zanos, T.P., 2020. Presenting characteristics, comorbidities, and outcomes among 5700 patients hospitalized with COVID-19 in the New York city area. JAMA.
Rodrigues, T.S., de Sa, K.S.G., Ishimoto, A.Y., Becerra, A., Oliveira, S., Almeida, L., Goncalves, A.V., Perucello, D.B., Andrade, W.A., Castro, R., Veras, F.P., Toller-Kawahisa, J.E., Nascimento, D.C., de Lima, M.H.F., Silva, C.M.S., Caetite, D.B., Martins, R.B., Castro, I.A., Pontelli, M.C., de Barros, F.C., do Amaral, N.B., Giannini, M.C., Bonjorno, L.P., Lopes, M.I.F., Santana, R.C., Vilar, F.C., Auxiliadora-Martins, M., Luppino-Assad, R., de Almeida, S.C.L., de Oliveira, F.R., Batah, S.S., Siyuan, L., Benatti, M.N., Cunha, T.M., Alves-Filho, J.C., Cunha, F.Q., Cunha, L.D., Frantz, F.G., Kohlsdorf, T., Fabro, A.T., Arruda, E., de Oliveira, R.D.R., Louzada-Junior, P., Zamboni, D.S., 2021. Inflammasomes are activated in response to SARS-CoV-2 infection and are associated with COVID-19 severity in patients. J. Exp. Med. 218.
Siu, K.L., Yuen, K.S., Castano-Rodriguez, C., Ye, Z.W., Yeung, M.L., Fung, S.Y., Yuan, S., Chan, C.P., Yuen, K.Y., Enjuanes, L., Jin, D.Y., 2019. Severe acute respiratory syndrome coronavirus ORF3a protein activates the NLRP3 inflammasome by promoting TRAF3-dependent ubiquitination of ASC. Faseb. J. 33, 8865–8877.
Stienstra, R., van Diepen, J.A., Tack, C.J., Zaki, M.H., van de Veerdonk, F.L., Perera, D., Neale, G.A., Hooiveld, G.J., Hijmans, A., Vroegrijk, I., van den Berg, S., Romijn, J., Rensen, P.C., Joosten, L.A., Netea, M.G., Kanneganti, T.D., 2011. Inflammasome is a central player in the induction of obesity and insulin resistance. Proc. Natl. Acad. Sci. U. S. A. 108, 15324–15329.
Sun, X., Liu, Y., Huang, Z., Xu, W., Hu, W., Yi, L., Liu, Z., Chan, H., Zeng, J., Liu, X., Chen, H., Yu, J., Chan, F.K.L., Ng, S.C., Wong, S.H., Wang, M.H., Gin, T., Joynt, G.M., Hui, D.S.C., Zou, X., Shu, Y., Cheng, C.H.K., Fang, S., Luo, H., Lu, J., Chan, M.T.V., Zhang, L., Wu, W.K.K., 2022. SARS-CoV-2 non-structural protein 6 triggers NLRP3-dependent pyroptosis by targeting ATP6AP1. Cell Death Differ.
Toldo, S., Bussani, R., Nuzzi, V., Bonaventura, A., Mauro, A.G., Cannata, A., Pillappa, R., Sinagra, G., Nana-Sinkam, P., Sime, P., Abbate, A., 2021. Inflammasome formation in the lungs of patients with fatal COVID-19. Inflamm. Res. 70, 7–10.
Tsuji, G., Hashimoto-Hachiya, A., Yen, V.H., Takemura, M., Yumine, A., Furue, K., Furue, M., Nakahara, T., 2020. Metformin inhibits IL-1beta secretion via impairment of NLRP3 inflammasome in keratinocytes: implications for preventing the development of psoriasis. Cell Death Dis. 6, 11.
Wang, Y.W., He, S.J., Feng, X., Cheng, J., Luo, Y.T., Tian, L., Huang, Q., 2017. Metformin: a review of its potential indications. Drug Des. Dev. Ther. 11, 2421–2429.
Wu, Z., McGoogan, J.M., 2020. Characteristics of and important lessons from the coronavirus disease 2019 (COVID-19) outbreak in China: summary of a report of 72314 cases from the Chinese center for disease control and prevention. JAMA.
Xu, H., Perez, R.D., Frey, T.R., Burton, E.M., Mannemuddhu, S., Haley, J.D., McIntosh, M.T., Bhaduri-McIntosh, S., 2019a. Novel replisome-associated proteins at cellular replication forks in EBV-transformed B lymphocytes. PLoS Pathog. 15, e1008228.
Xu, S., Zhou, Q., Fan, C., Zhao, H., Wang, Y., Qiu, X., Yang, K., Ji, Q., 2019b. Doxycycline inhibits NAcht Leucine-rich repeat Protein 3 inflammasome activation and interleukin-1beta production induced by Porphyromonas gingivalis-lipopolysaccharide and adenosine triphosphate in human gingival fibroblasts. Arch. Oral Biol. 107, 104514.
Yalcinkaya, M., Liu, W., Islam, M.N., Kotini, A.G., Gusarova, G.A., Fidler, T.P., Papapetrou, E.P., Bhattacharya, J., Wang, N., Tall, A.R., 2021. Modulation of the NLRP3 inflammasome by sars-CoV-2 envelope protein. Sci. Rep. 11, 24432.
Yang, F., Qin, Y., Wang, Y., Meng, S., Xian, H., Che, H., Lv, J., Li, Y., Yu, Y., Bai, Y., Wang, L., 2019. Metformin inhibits the NLRP3 inflammasome via AMPK/mTOR-dependent effects in diabetic cardiomyopathy. Int. J. Biol. Sci. 15, 1010–1019.
Yang, J., Zheng, Y., Gou, X., Pu, K., Chen, Z., Guo, Q., Ji, R., Wang, H., Wang, Y., Zhou, Y., 2020. Prevalence of comorbidities and its effects in coronavirus disease 2019 patients: a systematic review and meta-analysis. Int. J. Infect. Dis. 94, 91–95.
Zhang, Q., Bastard, P., Liu, Z., Le Pen, J., Moncada-Velez, M., Chen, J., Ogishi, M., Sabli, I.K.D., Hodeib, S., Korol, C., Rosain, J., Bilguvar, K., Ye, J., Bolze, A., Bigio, B., Yang, R., Arias, A.A., Zhou, Q., Zhang, Y., Onodi, F., Korniotis, S., Karpf, L., Philippot, Q., Chbihi, M., Bonnet-Madin, L., Dorgham, K., Smith, N., Schneider, W. M., Razooky, B.S., Hoffmann, H.H., Michailidis, E., Moens, L., Han, J.E., Lorenzo, L., Bizien, L., Meade, P., Neehus, A.L., Ugurbil, A.C., Corneau, A., Kerner, G., Zhang, P., Rapaport, F., Seeleuthner, Y., Manry, J., Masson, C., Schmitt, Y., Schluter, A., Le Voyer, T., Khan, T., Li, J., Fellay, J., Roussel, L., Shahrooei, M., Alosaimi, M.F., Mansouri, D., Al-Saud, H., Al-Mulla, F., Almourfi, F., Al-Muhsen, S.Z., Alsohime, F., Al Turki, S., Hasanato, R., van de Beek, D., Biondi, A., Bettini, L.R., D'Angio, M., Bonfanti, P., Imberti, L., Sottini, A., Paghera, S., Quiros-Roldan, E., Rossi, C., Oler, A. J., Tompkins, M.F., Alba, C., Vandernoot, I., Goffard, J.C., Smits, G., Migeotte, I., Haerynck, F., Soler-Palacin, P., Martin-Nalda, A., Colobran, R., Morange, P.E., Keles, S., Colkesen, F., Ozcelik, T., Yasar, K.K., Senoglu, S., Karabela, S.N., Gallego, C.R., Novelli, G., Hraiech, S., Tandjaoui-Lambiotte, Y., Duval, X., Laouenan, C., Clinicians, C.-S., Clinicians, C., Imagine, C.G., French, C.C.S.G., Co, V. C.C., Amsterdam, U.M.C.C., , Biobank, Effort, C.H.G., Niaid, U., Group, T.C.I., Snow, A.L., Dalgard, C.L., Milner, J., Vinh, D.C., Mogensen, T.H., Marr, N., Spaan, A. N., Boisson, B., Boisson-Dupuis, S., Bustamante, J., Puel, A., Ciancanelli, M., Meyts, I., Maniatis, T., Soumelis, V., Amara, A., Nussenzweig, M., Garcia-Sastre, A., Krammer, F., Pujol, A., Duffy, D., Lifton, R., Zhang, S.Y., Gorochov, G., Beziat, V., Jouanguy, E., Sancho-Shimizu, V., Rice, C.M., Abel, L., Notarangelo, L.D., Cobat, A., Su, H.C., Casanova, J.L., 2020. Inborn errors of type I IFN immunity in patients with life-threatening COVID-19. Science.
Zhang, W., Xie, X., Wu, D., Jin, X., Liu, R., Hu, X., Fu, Y., Ding, Z., Zhang, N., Cao, Y., 2017. Doxycycline attenuates leptospira-induced IL-1beta by suppressing NLRP3 inflammasome priming. Front. Immunol. 8, 857.